THE JOURNAL OF BIOLOGICAL CHEMISTRY VOL. 288, NO. 20, pp. 14200–14211, May 17, 2013
Published in the U.S.A.

Physical and Functional Interactions of a Monothiol Glutaredoxin and an Iron Sulfur Cluster Carrier Protein with the Sulfur-donating Radical *S*-Adenosyl-L-methionine Enzyme MiaB*

Received for publication, February 7, 2013, and in revised form, March 27, 2013 Published, JBC Papers in Press, March 29, 2013, DOI 10.1074/jbc.M113.460360

Sylvain Boutigny[‡], Avneesh Saini[‡], Edward E. K. Baidoo[§¶], Natasha Yeung[‡], Jay D. Keasling[§¶‖], and Gareth Butland[‡1]**

*From the [‡]Life Sciences Division and [§]Physical Biosciences Division, Lawrence Berkeley National Laboratory, Berkeley, California 94720, the Departments of [‖]Chemical Engineering and **Bioengineering, University of California, Berkeley, California 94720, and the [¶]Joint BioEnergy Institute, Emeryville, California 94608*

Background: MiaB requires constant regeneration of one of its iron sulfur clusters to perform multiple catalytic cycles.
Results: Accessory *Escherichia coli* iron sulfur cluster biosynthesis factors GrxD and NfuA physically interacts with MiaB and affects its activity *in vivo*.
Conclusion: GrxD and NfuA are functionally linked with MiaB.
Significance: GrxD and NfuA could be involved in the repair of the sacrificial cluster in MiaB.

The biosynthesis of iron sulfur (FeS) clusters, their trafficking from initial assembly on scaffold proteins via carrier proteins to final incorporation into FeS apoproteins, is a highly coordinated process enabled by multiprotein systems encoded in *iscRSUAhscBAfdx* and *sufABCDSE* operons in *Escherichia coli*. Although these systems are believed to encode all factors required for initial cluster assembly and transfer to FeS carrier proteins, accessory factors such as monothiol glutaredoxin, GrxD, and the FeS carrier protein NfuA are located outside of these defined systems. These factors have been suggested to function both as shuttle proteins acting to transfer clusters between scaffold and carrier proteins and in the final stages of FeS protein assembly by transferring clusters to client FeS apoproteins. Here we implicate both of these factors in client protein interactions. We demonstrate specific interactions between GrxD, NfuA, and the methylthiolase MiaB, a radical *S*-adenosyl-L-methionine-dependent enzyme involved in the maturation of a subset of tRNAs. We show that GrxD and NfuA physically interact with MiaB with affinities compatible with an *in vivo* function. We furthermore demonstrate that NfuA is able to transfer its cluster *in vitro* to MiaB, whereas GrxD is unable to do so. The relevance of these interactions was demonstrated by linking the activity of MiaB with GrxD and NfuA *in vivo*. We observe a severe defect in *in vivo* MiaB activity in cells lacking both GrxD and NfuA, suggesting that these proteins could play complementary roles in maturation and repair of MiaB.

The maturation of iron sulfur (FeS) cluster-containing proteins continues to be a subject of great interest due to the major roles played by FeS proteins in cellular biochemistry of organisms of all complexity from *Escherichia coli* to mammalian systems (1–5). Indeed, much is now known about the process surrounding initial cluster assembly on an FeS scaffold protein, the factors involved, and their interactions (4). Interactions between FeS-containing scaffold proteins and FeS carrier proteins acting downstream remain relatively poorly characterized, and the subsequent interactions of FeS carrier proteins, which interact with and transfer nascent FeS clusters to their target destination in client FeS apoproteins, have been analyzed in only a few targeted cases (6–8). In this work, we implicate the monothiol glutaredoxin GrxD and the FeS cluster carrier protein NfuA as physically and functionally interacting with the radical *S*-adenosylmethionine (AdoMet)[2]-dependent methylthiolase MiaB, indicating a potential role in enabling efficient turnover of this enzyme.

We have previously implicated the *E. coli* monothiol glutaredoxin GrxD as playing an as yet undefined role in FeS cluster biosynthesis in *E. coli* due to the severe synthetic lethality of a *grxD* mutation in combination with mutations of the Isc system, the major FeS cluster biosynthesis apparatus of the cell (9). GrxD can form FeS cluster-containing complexes as both a homodimer and a heterodimer with BolA (10, 11), a poorly characterized protein involved in cell morphology and resistance to stress (12). The GrxD homodimer and GrxD-BolA heterodimer complexes are both capable of intact transfer of their FeS cluster to the model client protein apoferredoxin (Fdx) *in*

* This work was supported, in whole or in part, by National Institutes of Health Grant GM088196 from the NIGMS. This work was also supported by the Director, Office of Science, of the United States Department of Energy under Contract DE-AC02-05CH11231 through an E. O. Lawrence Fellowship (to N. Y.).

[1] To whom correspondence should be addressed. Tel: 510-486-6905; Fax: 510-495-2723; E-mail: gpbutland@lbl.gov.

[2] The abbreviations used are: AdoMet, *S*-adenosylmethionine; Isc, iron sulfur cluster biosynthesis system; Suf, sulfur utilization factor biosynthesis system; Nif, nitrogen fixation biosynthesis system; i^6A, the modified nucleoside N^6-isopentenyl adenosine; ms^2i^6A, the modified nucleoside 2-methylthio-N^6-isopentenyl adenosine; Fdx, ferredoxin; Grx, glutaredoxin; SPA, Sequential peptide affinity; AcnB, aconitase B; ESI, electrospray mass ionization.

vitro. Other *in vitro* work with *Azotobacter vinelandii* has shown that the *A. vinelandii* Grx5 monothiol glutaredoxin can accept an FeS cluster from IscU and that *A. vinelandii* Grx-nif can act to transfer an FeS cluster to the A-type carrier protein *A. vinelandii* ^{Nif}IscA (13). However, the *in vivo* role for GrxD remains unknown, and the range of cellular processes impacted remains uncharacterized. One potential clue as to *in vivo* GrxD function in *E. coli* comes from protein-protein interaction data (14). Sequential peptide affinity (SPA) purification of native levels of GrxD-SPA and BolA-SPA affinity-tagged proteins revealed that although GrxD co-purified with only small amounts of BolA, the affinity purification of BolA resulted in the co-purification of GrxD and small quantities of several other proteins including MiaB (14, 15) and the recently characterized NfuA (8, 16).[3] These data therefore implicated GrxD (and/or BolA) and NfuA in *in vivo* binding of, and potential FeS cluster transfer to, a client FeS apoprotein in MiaB.

NfuA is necessary for adaptation to oxidative stress and iron starvation in *E. coli* and linked to aconitase A maturation in *A. vinelandii* (16, 17). Recent work demonstrated that NfuA acts as an FeS carrier protein that functions outside of defined Suf or Isc biosynthesis systems and is involved in maturation of aconitase B (AcnB) and the NuoG subunit of NADH dehydrogenase in *E. coli* (8). MiaB is a radical AdoMet enzyme involved in methylthiolation of a subset of tRNAs, a process required for their maturation (18, 19). The adenosine modification, 2-methylthio-N^6-isopentenyl adenosine (ms^2i^6A), is found at tRNA position 37 next to the anticodon. The first step of ms^2i^6A synthesis is catalyzed by MiaA and involves the addition of an isopentenyl group at the N^6 nitrogen of adenosine 37 (A-37) to produce isopentenyl adenosine (i^6A). The second step of the reaction is catalyzed by MiaB and consists of both sulfur insertion and methylation at position 2 of i^6A (15, 18–20). MiaB has been proposed to utilize AdoMet to generate a tRNA substrate for sulfur insertion. Sulfur insertion would then proceed, utilizing the auxiliary "nonradical AdoMet" 4Fe4S cluster as a sulfur source (21, 22). A second equivalent of AdoMet is then used to catalyze the methylation of the intermediate thio-N^6-isopentenyl adenosine group (s^2i^6A). The proposed catalytic mechanism of MiaB entails self-sacrifice and the use of one of its own iron sulfur clusters as a substrate, suggesting that the enzyme requires constant FeS cluster regeneration or repair to perform multiple turnovers. Our goal is to validate and characterize the physical interactions and intact FeS cluster transfer properties of GrxD and NfuA with MiaB and determine how these factors influence the methylthiolation activity of MiaB *in vivo*.

MATERIALS AND METHODS

Bacterial Strains and Plasmids—Plasmid vectors expressing N-terminal tagged *E. coli* His_6-MiaB (pET6HMiaB), His_6-NfuA (pET6HNfuA), His_6-SufA (pET6HSufA), His_6-ErpA (pET6HErpA), and His_6-IscA (pET6HIscA) were created by independently amplifying the *miaB*, *nfuA*, *sufA*, *erpA*, and *iscA* genes from *E. coli* BW25113 genomic DNA by PCR and subsequent cloning of the PCR product into a pET28(b) vector (Novagen) using NdeI and HindIII restriction sites incorporated into the oligonucleotide primers. Plasmid constructs were freshly transformed into *E. coli* BL21(DE3) prior to use. Plasmid constructs to overproduce GrxD, BolA, and Fdx and their use were described previously (10).

MiaB C157A/C161A/C164A Mutant—The MiaB C157A/C161A/C164A triple mutant was constructed by amplifying the 5′ part of the gene (nucleotides 1–490) with 5′-gggaatccatatgaccaaaaaactcc (introduction of a NdeI restriction site) and 5′-taggatcgtacgtggcatatttattggcgccttccatgatggagac (introduction of a BsiWI restriction site and the C157A and C161A mutations) (fragment 1) and the 3′ part of the gene with 5′-gtgaaacgtacgctgtggtgccttacacccgtg (introduction of a BsiWI restriction site and the C164A mutation) and 5′-ccgatcgaattcaccgac (contains a EcoRV restriction site) (fragment 2). The restriction sites are underlined.

The PCR DNA fragment 1 was digested using NdeI and BsiWI, and the DNA fragment 2 was digested using BsiWI and EcoRV. The two digested pieces of DNA were ligated in a pET6HMiaB backbone digested by NdeI and EcoRV. The ligation product was transformed into DH5α cells, positive clones were verified by DNA sequencing, and constructs were designated pET6HMiaB3CA.

Protein Expression and Purification—All proteins were overproduced and purified to homogeneity exactly as described previously for GrxD (10) with the following modification: gel filtration buffer contained 200 mM NaCl instead of 150 mM KCl.

Protein Cleavage—His-tagged proteins were cleaved using the Novagen cleavage capture kit according to the specifications of the manufacturer.

Circular Dichroism (CD)—CD spectra (100 μM protein) were collected on a JASCO J-815 spectropolarimeter equipped with a Peltier temperature controller and stirring module. Apoprotein spectra were collected aerobically. Reconstituted proteins were prepared in an anaerobic chamber and analyzed in sealed cuvettes. CD spectra were recorded with stirring under the following conditions: temperature = 25 °C; digital integration time = 2 s; bandwidth = 1 nm; accumulations = 3; data pitch = 0.1 nm; and scan speed = 50 nm/min.

tRNA Extraction—The tRNA extraction protocol was adapted from a previously described procedure (19) with the following modifications. *E. coli* strains to be analyzed were grown for 24 h at 37 °C in 1 liter of LB medium containing the appropriate antibiotic. The cells were then centrifuged and resuspended in 20 ml of 0.3 M sodium acetate, pH 4.5, 10 mM EDTA, flash-frozen in liquid nitrogen, and stored at −80 °C until use. Cells were lysed, and RNA was separated from cell debris and proteins using phenol saturated with 300 mM sodium acetate, pH 4.5, 10 mM EDTA. After purification on a NucleoBond AX 2000 column and a washing step, the pellet containing tRNAs was resuspended in water, snap-frozen, and stored at −80 °C. tRNAs (300 μg) were digested for 16 h at 37 °C in 20 mM ammonium acetate, pH 5.1, in the presence of 30 units of nuclease P1 (Sigma) and 0.5 mM $ZnSO_4$. Tris-HCl, pH 7.4, was added to reach a concentration of 50 mM with 15 units of alkaline phosphatase (Sigma) and incubated for 4 h at 37 °C. Methanol was added to reach a concentration of 50% (V/V), and the solution was applied to a 3K Centricon (Milli-

[3] N. Yeung, unpublished data.

pore). The pass-through containing the digested nucleosides was saved, lyophilized, and resuspended in 50% MeOH.

Analysis of Nucleosides from tRNAs by Liquid Chromatography-Electrospray Ionization-Time-of-flight Mass Spectrometry (LC-ESI-TOF-MS)—The solvents and chemicals used for these analyses were of HPLC grade (Honeywell Burdick & Jackson). Liquid chromatographic separation of nucleosides was conducted at 50 °C with a Kinetex XB-C18 reversed phase column (100-mm length, 3-mm internal diameter, 2.6-μm particle size; Phenomenex) using a 1200 series ZORBAX rapid resolution high-performance liquid chromatography (HPLC) system (Agilent Technologies). The injection volume for each measurement was 8 μl. The mobile phase was composed of 10 mM ammonium acetate (Sigma-Aldrich) in water (solvent A) and 10 mM ammonium acetate in 90% acetonitrile and 10% water (solvent B). The mobile phases were made up from a stock solution of 100 mM ammonium acetate and 0.7% formic acid (Sigma-Aldrich) in water. Nucleosides were separated with the following gradient: 20–100% B for 5 min, held at 100% B for 1 min, 100–20% B for 0.5 min, held at 20% B for 4 min. A flow rate of 0.4 ml/min was used throughout. Nucleosides were observed via diode array detection at a UV absorbance wavelength of 260 nm. The HPLC system was coupled to an Agilent Technologies 6210 TOF MS. Drying and nebulizing gases (*i.e.* nitrogen) were set to 12 liters/min and 25 pounds/in^2, respectively, and a drying gas temperature of 320 °C was used throughout. ESI was conducted in the positive ion mode. ESI-MS experiments were carried out with a capillary voltage of 3.5 kV at 0.86 spectra/s for the detection of $[M + H]^+$ ions. Data acquisition and processing were performed by the Agilent MassHunter software package.

Surface Plasmon Resonance—Surface plasmon resonance experiments were performed on a Biacore T100 (GE Healthcare). The His tag-free protein of interest was covalently immobilized to the carboxymethylated dextran matrix on a CM5 sensor chip (GE Healthcare) via primary amino groups using the amine-coupling protocol (GE Healthcare). Purified and tag-free GrxD, NfuA, MiaB, BolA, SufA, ErpA, and IscA were injected at various concentrations. All experiments were performed at a flow rate of 20 μl/min in 100 mM Tris, pH 8, 100 mM NaCl, 2 mM dithiothreitol (DTT), 0.05% Tween 20. Binding of analyte to MiaB at equilibrium was plotted against analyte concentration, and the Biacore T100 evaluation software (Biacore) program was used to create a nonlinear curve fit of the data.

Analytical Gel Filtration—Analytical gel filtration was performed on a Superdex 75 PC 3.2/30 column connected to an Ettan LC system (GE Healthcare). The column was equilibrated with gel filtration buffer (50 mM Tris-HCl, pH 8.0, 150 mM KCl, 2 mM DTT, 1.5 mM glutathione) unless otherwise specified. Air-sensitive samples were taken out of an anaerobic chamber (Coy Laboratory Products) in gastight syringes and loaded immediately onto the column. Calibration was performed with the low molecular weight gel filtration calibration kit (GE Healthcare).

Reconstitution of the FeS Clusters in MiaB—Apo-MiaB (150 μM) was incubated in an anaerobic chamber at 25 °C with 0.014 eq of IscS and 5 mM L-cysteine in reconstitution buffer (100 mM Tris-HCl, pH 8, 100 mM NaCl, 5 mM DTT). All components were degassed before introduction into an anaerobic chamber. Reconstitution reactions were set up to include all components except iron and incubated with constant stirring for 20 min. Reconstitution was initiated by the slow addition of 20 eq of ammonium iron (III) sulfate (Sigma-Aldrich). The protein mixture was allowed to mix for a further 2 h before application onto a Q-Sepharose column equilibrated with 50 mM Tris-HCl, pH 8. The column was rinsed with 5 column volumes of Tris-HCl, pH 8, and the protein was eluted using 50 mM Tris-HCl, pH 8, 500 mM NaCl.

Reconstitution of the FeS Cluster in GrxD—Apo-GrxD or His-tagged apo-GrxD was reconstituted exactly as described previously (10).

Reconstitution of the FeS Cluster in NfuA—Apo-NfuA (100 μM) was incubated in an anaerobic chamber at 25 °C with 0.05 eq of IscS and 2 mM L-cysteine in reconstitution buffer. After incubation for 20 min with constant stirring, 2 mM ammonium iron (III) sulfate was slowly added. The protein mixture was allowed to mix for a further 1 h before application onto a Q-Sepharose column equilibrated with 50 mM Tris-HCl, pH 8. The column was rinsed with 5 column volumes of 50 mM Tris-HCl, pH 8, and the protein was eluted using 50 mM Tris-HCl, pH 8, 500 mM NaCl.

Affinity Co-purification Assay—Apo-MiaB (100 μM) was incubated for 1 h in 50 mM Tris-HCl, pH 8, 100 mM NaCl, 5 mM DTT with the His-tagged bait protein. Samples were then applied to a 1-ml HisTrap affinity column (GE Healthcare) and washed five times with 1 ml of buffer containing 50 mM Tris-HCl, pH 8, 100 mM NaCl, 5 mM DTT, and 40 mM imidazole to remove unbound MiaB. Bound proteins were eluted in 0.5-ml fractions with buffer containing 50 mM Tris-HCl, pH 8, 100 mM NaCl, 5 mM DTT, and 500 mM imidazole. Proteins present in each fraction were analyzed by SDS-PAGE. When GrxD was used as a bait, 2.5 mM glutathione was added to all the buffers listed above.

Analysis of FeS Transfer—Apo-MiaB (100 μM) was incubated with either reconstituted His-tagged holo-GrxD or reconstituted His-tagged holo-NfuA (200 μM) as described in the affinity co-purification assay and separated using a 1-ml HisTrap affinity column. Separation was performed as described in the affinity co-purification assay with the following modifications. Washes were made in a buffer containing 20 mM imidazole, and elution fractions were 1 ml. Proteins present in each fraction were analyzed by SDS-PAGE and by UV-visible spectrophotometry (Agilent HP 8453 spectrophotometer). When GrxD was used, 2.5 mM glutathione was added to all the buffers listed above.

Knock-out Mutants—E. coli single gene deletion mutants were taken from the KEIO collection (23). The *E. coli nfuA/grxD* double mutant (SB5068) was constructed by mutagenesis of *grxD* in an *nfuA* background according to the procedure previously described (24). Primer sequences used for mutagenesis are available on request.

RESULTS

MiaB from E. coli Binds Two 4Fe4S Clusters—Biochemical and spectroscopic characterization of MiaB from *Thermotoga maritima* had shown that the protein binds two 4Fe4S clusters

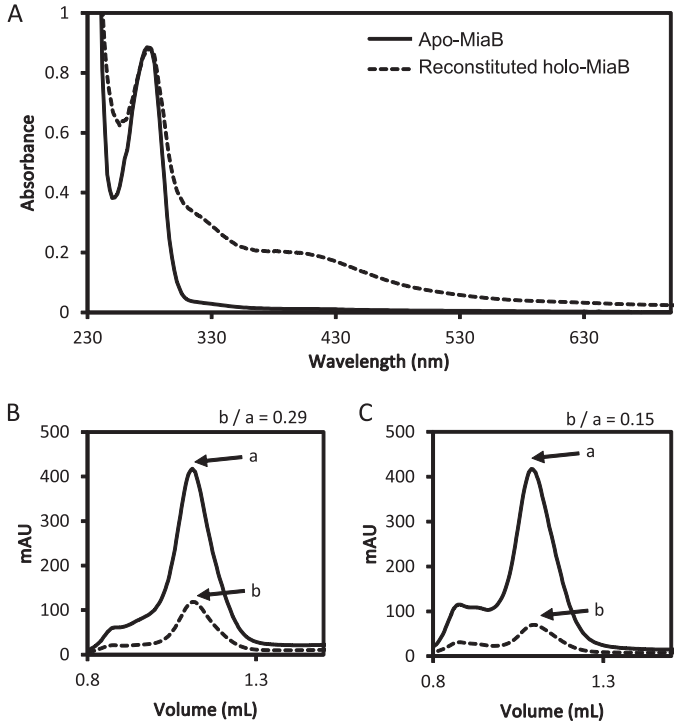

FIGURE 1. **UV-visible analysis of apo- and holo-MiaB and gel filtration comparison of holo-MiaB with holo-MiaB C157A/C161A/C164A.** *A*, UV-visible spectra of apo-MiaB (*solid line*) and reconstituted holo-MiaB (*dashed line*). *mAU*, milliabsorbance units. *B* and *C*, gel filtration analysis after reconstitution of MiaB (*B*) and MiaB C157A/C161A/C164A (*C*). Elution profiles followed at 280 nm are indicated by a *solid line*, and elution profiles followed at 414 nm are indicated by a *dashed line*. The ratio of the maximal peak absorption at 414 nm divided by the maximal peak absorption at 280 nm (indicated by the *arrows* marked with *b* and *a*) was 0.29 for WT MiaB and 0.15 for MiaB C157A/C161A/C164A. The spectra were normalized to identical total protein concentration.

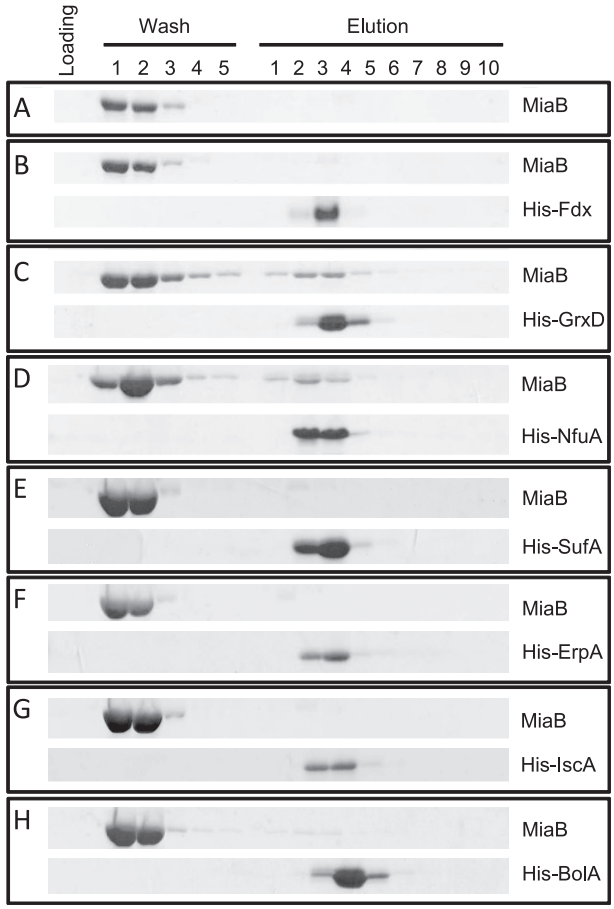

FIGURE 2. **Analysis of MiaB affinity co-purification with potential interacting protein partners.** *A–H*, Apo-MiaB (100 μM) was incubated with: no His-tagged protein (*A*), 100 μM His-tagged Fdx (*B*), 100 μM His-tagged GrxD (*C*), 100 μM His-tagged NfuA (*D*), 100 μM His-tagged SufA (*E*), 100 μM His-tagged ErpA (*F*), 100 μM His-tagged IscA (*G*), and 100 μM His-tagged BolA (*H*). Samples were applied to a 1-ml HisTrap affinity column and washed as described under "Materials and Methods." Fractions were analyzed by SDS-PAGE.

(25). However, previous work indicated that MiaB from *E. coli* contained only a single FeS cluster (15). To address this discrepancy, we reconstituted the FeS cluster(s) in *E. coli* MiaB. After reconstitution, an A_{414}/A_{280} ratio of 0.29 was obtained, which is very similar to that reported previously (25) (Fig. 1, *A* and *B*). To confirm the presence of a second cluster in *E. coli* MiaB, we targeted three cysteine residues located at positions 157, 161, and 164, which are conserved in the radical AdoMet enzyme family (21) and have been shown to be responsible for binding the radical AdoMet FeS cluster in *T. maritima* MiaB (25). Following reconstitution of the MiaB C157A/C161A/C164A mutant, the protein displayed an A_{414}/A_{280} ratio of 0.151, consistent with only one 4Fe4S cluster being reconstituted (Fig. 1*C*). Taken together, these results indicate that MiaB from *E. coli* can also bind two 4Fe4S clusters.

MiaB Directly Interacts with GrxD and NfuA—SPA purification data previously indicated that *E. coli* GrxD and BolA co-purify with each other, and FeS cluster-containing GrxD (± BolA) complexes were biochemically characterized (10). Mass spectrometry data also identified MiaB and NfuA as minor components of GrxD-SPA and BolA-SPA affinity-purified complexes (14).[3] We therefore sought to investigate the potential interaction of MiaB with GrxD, BolA, and NfuA using qualitative and quantitative approaches.

Affinity Co-purification of MiaB with GrxD and NfuA—To validate the potential interaction between the putative FeS cluster biosynthesis factors GrxD and NfuA and the FeS cluster client protein MiaB, a series of affinity co-purification experiments was performed. Untagged MiaB was incubated with potential His-tagged partner proteins, and the mixture was applied to a HisTrap column (Fig. 2). As expected, MiaB alone was not retained by the nickel-nitrilotriacetic acid resin. The same pattern was observed after MiaB was incubated with ferredoxin, an FeS protein not known to interact with MiaB, and His-Fdx eluted alone upon the addition of a high amount of imidazole. However, significant changes were observed in the elution profile of MiaB after incubation with His-GrxD or His-NfuA. The elution of MiaB is stretched over additional wash steps, and a portion of the protein co-elutes with either GrxD or NfuA upon the addition of a high concentration of imidazole. The reverse experiment (His-tagged MiaB mixed with untagged partner) leads to the same results (data not shown). To show the specificity of the interaction between MiaB and GrxD/NfuA, additional co-purification experiments were performed with BolA and three known *E. coli* A-type carrier proteins, SufA, IscA, and ErpA (Fig. 2). A very small amount of MiaB was observed to co-purify with BolA, suggesting a weak association; however, no MiaB was detected as co-purifying

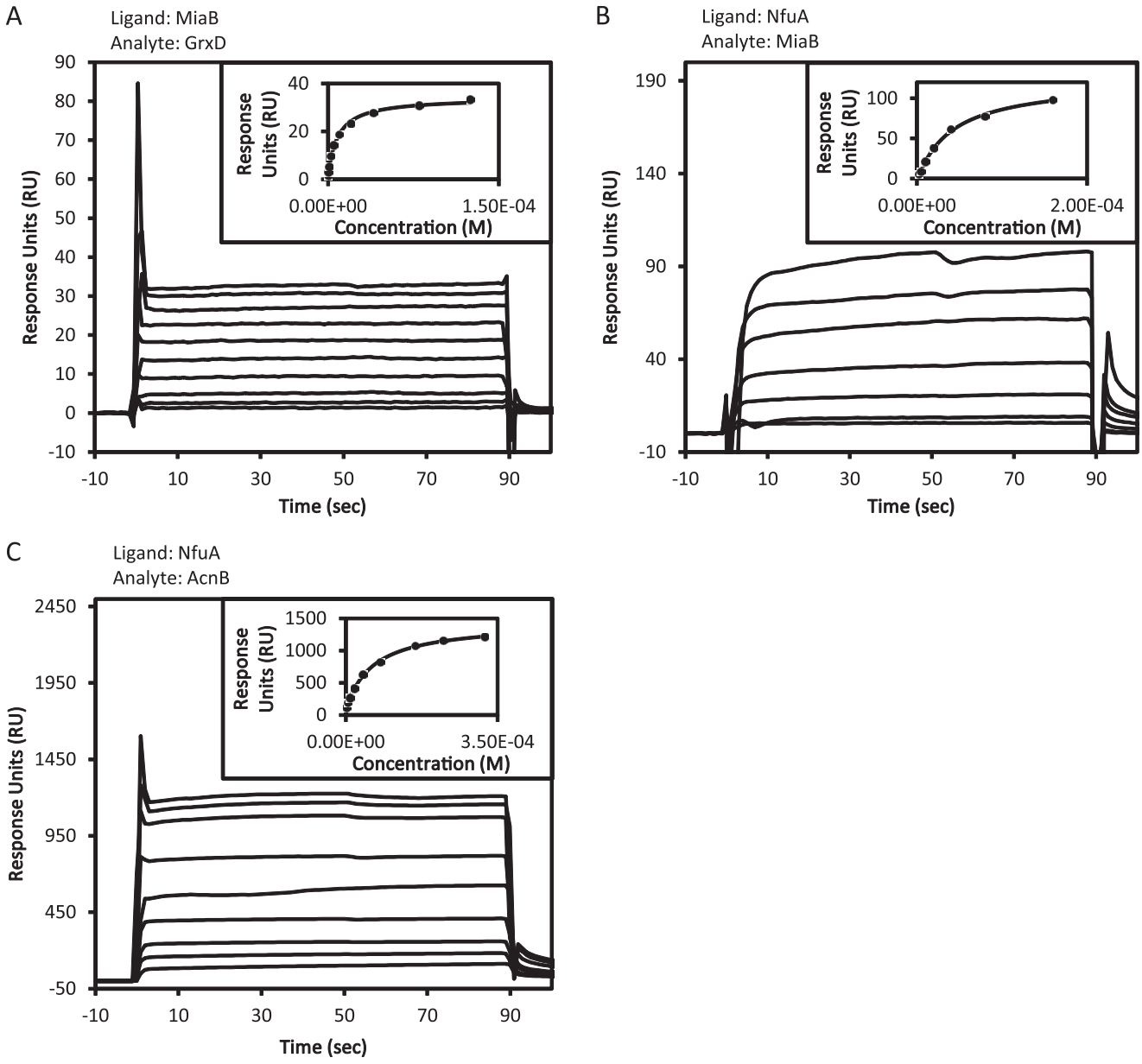

FIGURE 3. **Interaction of GrxD and NfuA with MiaB and NfuA with AcnB by surface plasmon resonance.** *A*, SPR sensorgram of the binding of 0.25, 0.5, 1, 2.5, 5, 10, 20, 40, 80, and 125 μM apo-GrxD to immobilized apo-MiaB on a CM5 chip. *Inset*: affinity curve of GrxD flowing on MiaB. The measured K_D for this experiment is 8.6 μM. The K_D obtained for three independent experiments was 12.0 $\pm$ 2.6 μM. *B*, SPR sensorgram of the binding of 2.5, 5, 10, 20, 40, 80, and 160 μM MiaB to immobilized NfuA on a CM5 chip. *Inset*: affinity curve of MiaB flowing on NfuA. The measured K_D for this experiment is 41.0 μM. The K_D obtained for eight independent experiments was 44.0 $\pm$ 5.2 μM. *C*, SPR sensorgram of the binding of 2.5, 5, 10, 20, 40, 80, 160, 225, and 320 μM AcnB to immobilized NfuA on a CM5 chip. *Inset*: affinity curve of AcnB flowing on NfuA. The measured K_D for this experiment is 60.0 μM. The K_D obtained for three independent experiments was 54.6 $\pm$ 8.3 μM.

with SufA, IscA, or ErpA. These results indicate that MiaB is being retained on the column by only His-GrxD and His-NfuA, consistent with specific physical interactions occurring between these proteins.

Quantitative Binding of GrxD and NfuA with MiaB by Surface Plasmon Resonance (SPR)—SPR is routinely used to detect and quantify the affinity of an interaction between protein pairs. To confirm the physical interactions observed in the co-purification assays, MiaB, GrxD, and NfuA were purified as described, and binding between apo-MiaB and apo-GrxD or apo-NfuA was probed by SPR. Apo-MiaB was covalently coupled to the chip surface and resonance was monitored, whereas increasing amounts of apo-GrxD were passed over the chip. A dose-response curve was obtained where an increase in response units was observed with increasing concentrations of apo-GrxD (Fig. 3*A*). Results obtained from three independent experiments indicate that apo-GrxD interacts with apo-MiaB with a K_D of 12.0 $\pm$ 2.6 μM. The interaction between apo-MiaB and apo-NfuA was also confirmed and quantified by passing apo-MiaB over an apo-NfuA-coupled chip surface. The K_D for apo-NfuA binding to apo-MiaB was 44.0 $\pm$ 5.2 μM (Fig. 3*B*). The relevance of the interaction between NfuA and MiaB was confirmed using AcnB, a reported client of NfuA, as a standard (8). The affinity of the AcnB/NfuA interaction was determined

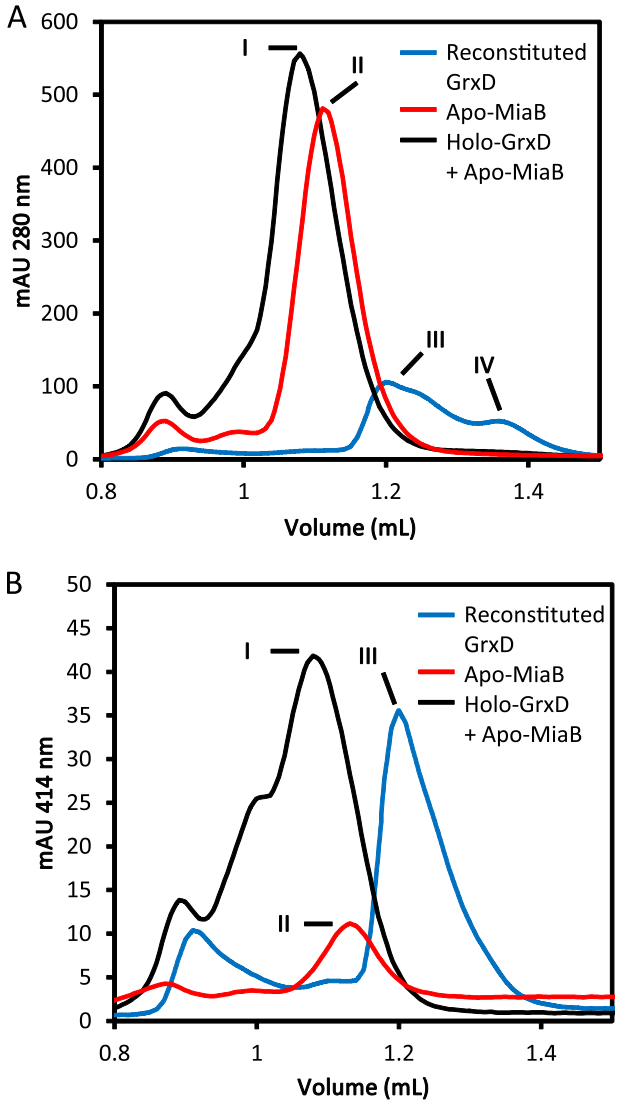

FIGURE 4. **Analysis of complex formation between GrxD and MiaB.** *A* and *B*, elution profile monitored at 280 (*A*) and 414 nm (*B*) from reconstituted holo-GrxD, apo-MiaB, and the incubation of apo-MiaB with reconstituted holo-GrxD. Each protein was present at 100 μM. Peak labels (*I–IV*) were assigned from higher to lower apparent molecular size and are described under "Results." *mAU*, milliabsorbance units.

to be K_D = 54.6 ± 8.3 μM by SPR (Fig. 3*C*). In contrast, no interaction was observed between MiaB and ErpA, IscA, or SufA (data not shown). These results were consistent with those obtained via affinity co-purification. In the case of BolA, no interaction with MiaB was observed by SPR despite indication of a weak interaction by co-purification. These data highlight the need to utilize multiple approaches to identify and validate protein interactions.

Complex Formation between GrxD and MiaB—To uncover the nature of the complex(es) formed by the interaction of GrxD with MiaB, we incubated the purified proteins together under multiple conditions and analyzed the apparent molecular mass and FeS cluster content by analytical gel filtration (Fig. 4). MiaB eluted as a single major peak with an apparent molecular mass of 51.7 ± 1.3 kDa (expected molecular mass = 53.6 kDa) (Fig. 4*A*, *peak II*) and a minor peak corresponding to the void volume of the column, which may indicate a MiaB protein aggregate. FeS cluster reconstituted GrxD migrated as a mixture of dimeric holo-protein (apparent molecular mass: 37.9 ± 2.6 kDa) and monomeric apoprotein (apparent molecular mass: 17.5 ± 1.7 kDa), consistent with previously published data (Fig. 4*A*, *peaks III* and *IV*, respectively) (10). Following incubation of apo-MiaB with reconstituted GrxD at a 1:1 ratio, the resulting mixture was analyzed by gel filtration. The 280 nm elution profile was found to contain only two resolved species by gel filtration. The major protein species was present in a peak corresponding to an apparent molecular mass of 60.0 ± 2.3 kDa (Fig. 4*A*, *peak I*), with an additional minor high molecular mass species present in void volume. Strikingly, both of the peaks corresponding to GrxD (Fig. 4*A*, *peaks III* and *IV*) were not observed in the 280 nm absorbance profile. We believe these data are consistent with the 60-kDa peak corresponding to a mixture of a MiaB-GrxD complex and MiaB alone. The absence of both apo-GrxD and holo-GrxD from the elution profile suggests that both forms of GrxD are being trapped by MiaB and that this interaction does not depend on the presence of an FeS cluster. These observations are supported by analysis of the 414 nm elution profile (Fig. 4*B*). Here the presence of the FeS cluster in the profile of GrxD alone at 37.9 ± 2.6 kDa (Fig. 4*B*, *peak III*) is completely absent from the profile of the MiaB and GrxD mixture. Noticeably, we observed a correspondingly large increase in FeS cluster content (11.6–41.8 milliabsorbance units) and a slight shift to higher mass at 60.0 ± 2.3 kDa (Fig. 4*B*, *peak I*) when comparing MiaB in the presence of GrxD to MiaB alone (51.7 ± 1.3 kDa) (Fig. 4*B*, *peak II*). These results are consistent with an intact holo-GrxD-[2Fe2S] dimer binding and forming a complex with apo-MiaB.

GrxD Does Not Transfer an FeS Cluster to Apo-MiaB—As the above results provide evidence for holo-GrxD binding to apo-MiaB, we investigated whether GrxD could transfer its cluster to apo-MiaB. His-tagged reconstituted holo-GrxD was incubated with apo-MiaB (1 MiaB:2 GrxD). After separation of GrxD from MiaB on a HisTrap affinity column, the purification fractions were analyzed by SDS-PAGE and UV-visible spectroscopy. SDS-PAGE indicated that the wash fractions contained only MiaB and that the elution fractions contained a mixture of GrxD and MiaB (Fig. 5*A*). Although the MiaB-containing wash fractions did not show the presence of an FeS cluster (Fig. 5*B*), the elution fractions, containing both GrxD and MiaB, displayed UV-visible spectra typical of a 2Fe2S cluster (Fig. 5*C*). The apparent decrease of FeS cluster content in the elution fractions is likely be due to the additional presence of MiaB protein and not due to true FeS cluster degradation or transfer (Fig. 5*C*). Additional experiments to ascertain whether the FeS cluster in the GrxD/MiaB mixture remained present in GrxD or had been transferred to MiaB were performed using CD (Fig. 5*D*). The spectrum of reconstituted GrxD is consistent with previously published results (10). The CD spectra of holo-GrxD showed three maxima at 316, 473, and 564 nm as well as two minima at 355 and 525 nm. The CD spectra of apo- and holo-MiaB were also recorded. As expected, apo-MiaB did not show any features in the visible region (data not shown); however, the spectrum of holo-MiaB contained spectral features (a minimum at 425 nm and maxima at 316 and 500 nm) consistent with the presence of 4Fe4S clusters (26). Upon incubation of

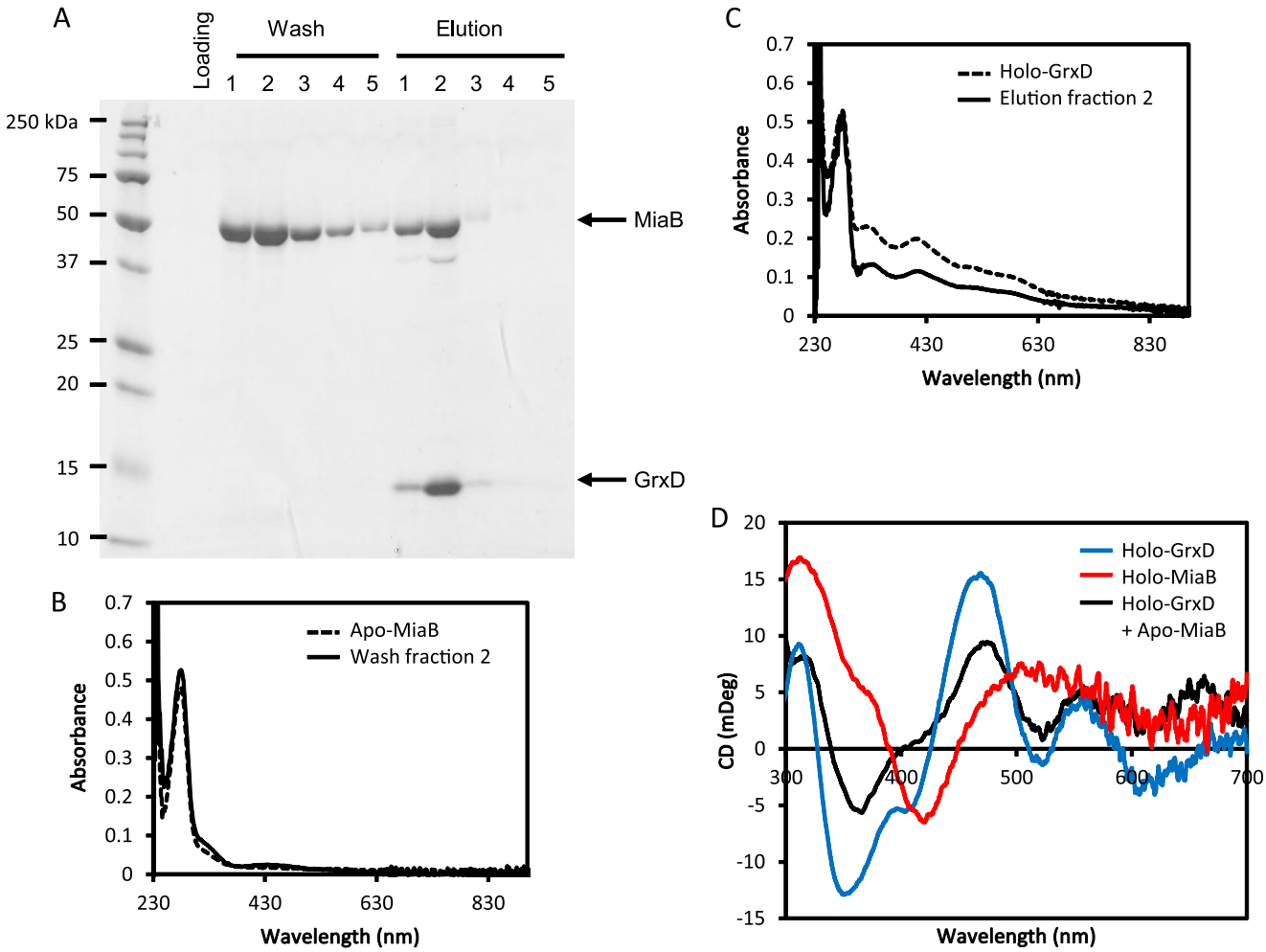

FIGURE 5. **GrxD does not transfer an FeS cluster to apo-MiaB.** *A*, SDS-PAGE analysis of the fractions collected after incubation and HisTrap separation of reconstituted holo-His-tagged GrxD (200 μM) and apo-MiaB (100 μM). *B*, UV-visible spectra of apo-MiaB (*dashed line*) and the second wash fraction (*solid line*). *C*, UV-visible spectra of reconstituted holo-GrxD (*dashed line*) and the second elution fraction (*solid line*). *D*, CD spectra of 100 μM holo-GrxD, 100 μM holo-MiaB, and 100 μM holo-GrxD after 1 h of incubation with 100 μM apo-MiaB. UV-visible spectra were normalized to identical total protein concentration (absorbance at 280 nm). *mDeg*, millidegrees.

holo-GrxD with apo-MiaB, we observed an overall decrease of the ellipticity of the CD spectrum of the mixture. However, the new spectrum is characteristic of holo-GrxD only. Taken together, these results indicate that GrxD physically interacts with apo-MiaB but retains, and does not transfer, its FeS cluster to the apoprotein under these conditions.

As a control, we also tested the ability of GrxD to transfer an FeS cluster to NfuA. Upon incubation of holo-GrxD with apo-NfuA, no spectroscopic changes were observed, and no FeS cluster transfer to, and accumulation in, NfuA was detected after gel filtration (data not shown).

NfuA Binds and Can Transfer a 4Fe4S Cluster to Apo-MiaB—The complex formed by MiaB incubated with holo-NfuA was also characterized using analytical gel filtration (Fig. 6*A*). Apo-MiaB eluted as described previously (Fig. 4*A*, *peak II* and Fig. 6*A*, *peak II*), and His-tagged apo-NfuA eluted at 29.5 ± 1.4 kDa (Fig. 6*A*, *peak III*) (expected molecular mass: 23.1 kDa). Following incubation of equimolar concentrations of apo-MiaB and apo-NfuA, gel filtration analysis revealed the presence of a single major peak at 62.2 ± 1.3 kDa (Fig. 6*A*, *peak I*) and the concomitant absence of a peak attributable to apo-NfuA. The major peak is shifted to higher apparent molecular mass when compared with MiaB alone, consistent with the formation of an MiaB-NfuA complex.

Potential transfer of the FeS cluster from NfuA to MiaB was monitored by incubating apo-MiaB with His-tagged reconstituted holo-NfuA. The sample was then applied to a HisTrap affinity column to permit separation of MiaB and NfuA. Fractions were analyzed by SDS-PAGE and revealed that only MiaB was present in the wash fractions, whereas elution fractions contained predominantly His-NfuA and a readily detectable amount of MiaB (Fig. 6*B*). Significantly, the UV-visible spectrum (Fig. 6*C*) of the second wash fraction, shown to contain only MiaB, had increased FeS cluster content when compared with apoprotein of the same concentration. Concomitantly, the UV-visible spectrum of the second elution fraction revealed a dramatic decrease of FeS cluster content in NfuA (Fig. 6*D*). These data support our observations of a MiaB-NfuA interaction (Fig. 2 and Fig. 3*B*) and further indicate that NfuA has transferred its 4Fe4S cluster to MiaB. To confirm that NfuA was capable of complete maturation of MiaB and insertion of 4Fe4S clusters to both radical SAM and UPF0004 domains, we

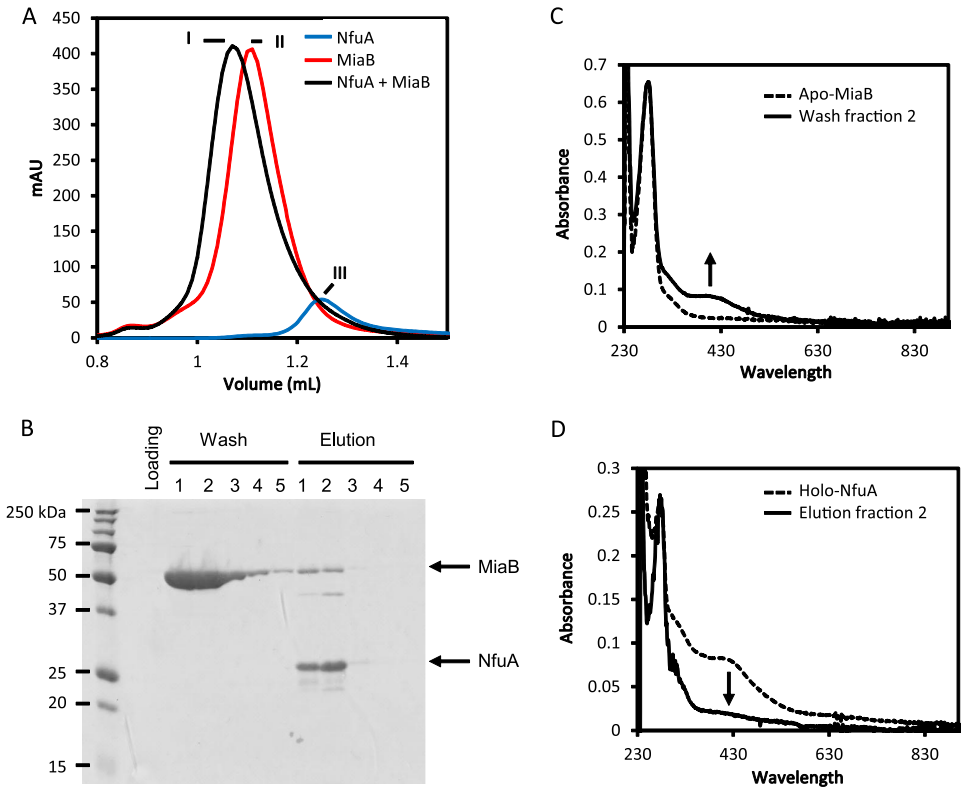

FIGURE 6. **Complex formation and FeS cluster transfer analysis of the interaction between NfuA and MiaB.** *A*, analysis of complex formation between NfuA and MiaB. Gel filtration elution profiles were recorded at 280 nm for apo-MiaB (*red*), apo-NfuA (*blue*), and apo-NfuA + apo-MiaB (*black*). Each protein was present at a concentration of 100 μM. Peak labels (*I–III*) were assigned from higher to lower apparent molecular size and are described under "Results." *mAU*, milliabsorbance units. *B*, SDS-PAGE analysis of the fractions collected after incubation and HisTrap separation of reconstituted His-tagged holo-NfuA (200 μM) and apo-MiaB (100 μM). *C*, UV-visible spectra of apo-MiaB (*dashed line*) and the second wash fraction (*solid line*). *D*, UV-visible spectra of reconstituted holo-NfuA (*dashed line*) and the second elution fraction (*solid line*). UV-visible spectra were normalized to identical total protein concentration (absorbance at 280 nm).

assayed the ability of NfuA to transfer its cluster to the MiaB C157A/C161A/C164A mutant. After incubation of an excess of His-tagged holo-NfuA with apo-C157A/C161A/C164A MiaB and separation of the two proteins using a HisTrap column, we observed UV-visible spectra of the C157A/C161A/C164A MiaB wash fractions consistent with the binding of a 4Fe4S cluster (data not shown). These results were almost identical to those reported for WT MiaB (Fig. 6) and indicate that NfuA is capable of transferring 4Fe4S clusters intact to both binding sites in MiaB.

NfuA and GrxD Have an Effect on the Activity of MiaB in Vivo—MiaB is involved in the methylthiolation of a subset of tRNAs (18, 20). To further link GrxD and NfuA to MiaB function and activity *in vivo*, tRNA analysis was performed. More specifically, tRNA was isolated and digested, and both fully modified nucleoside (ms^2i^6A) and partially modified nucleoside (i^6A) were quantified using reverse phase HPLC coupled to a mass spectrometer to determine the ms^2i^6A/i^6A ratio. The analysis of tRNAs from *E. coli* BW25113 indicated that there was 6.53 ± 0.44 times more ms^2i^6A than i^6A (Fig. 7*A*). This result is consistent with previously published data (27). Observed differences between ms^2i^6A/i^6A ratios reported here and elsewhere can be explained by the strong influence of growth medium used to culture *E. coli* as well as the method of tRNA preparation and analysis (28, 29). In this work, nucleosides were identified by LC-ESI-TOF-MS and quantified by HPLC-UV, which we believe is a more quantitative measure than a number of spectral counts by the mass spectrometer. As expected, the *miaB* mutant had an ms^2i^6A/i^6A ratio of 0.03 ± 0.04 as methylthiolation is blocked and no ms^2i^6A is produced in that strain. Interestingly, analysis of the ms^2i^6a/i^6a ratio in a *grxD* mutant showed a ratio of 5.90 ± 0.86, within an experimental margin of error. A ratio of 4.99 ± 0.51 was observed in an *nfuA* mutant, indicating a slight but significant impairment in ms^2i^6a production in this latter strain. In contrast, a *bolA* mutant showed a slight increase of the ms^2i^6a/i^6a ratio to 7.62 ± 0.64. A significant difference in the ms^2i^6A/i^6A ratio was obtained in an *nfuA*/*grxD* double mutant that showed a 5-fold decrease when compared with the wild type with an ms^2i^6A/i^6A ratio of 1.32 ± 0.08. The observed decrease in the ms^2i^6A/i^6A ratio corresponds to a significant impairment of MiaB activity in the *nfuA*/*grxD* double mutant (*cf.* either single mutant strain). These results strongly support the specific physical interaction and FeS cluster transfer data linking GrxD and NfuA to MiaB function.

Genetic Interaction between GrxD and NfuA—Growth curves made in LB medium on strains used for the nucleoside quantification did not display any significant differences between *E. coli* BW25113 and *miaB*, *bolA*, *grxD*, and *nfuA* mutants (Fig. 7*B*). In contrast, the *nfuA*/*grxD* double mutant displayed an impaired growth rate when compared with BW25113 and both *nfuA* and *grxD* single mutants. However, it should be noted that after a 24-h incubation, the cell density was approximately the same in all the strains tested (data not

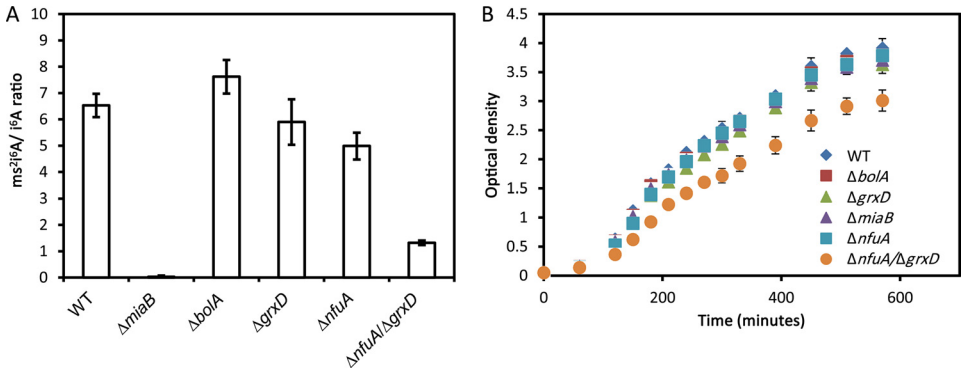

FIGURE 7. **HPLC-LC analysis of modified nucleosides present in tRNA and growth curves of the strains used for the tRNA analysis.** *A*, the ratio of ms^2i^6A/i^6A modified nucleosides present in *E. coli* BW25113 (*WT*) total tRNA and corresponding *miaB*, *bolA*, *grxD*, *nfuA*, and *nfuA/grxD* double mutant strains was obtained after UV quantification of ms^2i^6A and i^6A nucleosides present in total tRNA digests. Data represent results from three independent experiments using three independent mutant isolates. *B*, *E. coli* BW25113 (*WT*), *bolA*, *grxD*, *miaB*, *nfuA*, and *nfuA*/grxD mutants were grown in LB for 24 h. The optical density at 600 nm of the cultures was monitored over 24 h. The average of the A_{600} obtained by three independent experiments ± the S.D. is plotted.

shown). These results are indicative of an aggravating genetic interaction between *grxD* and *nfuA*.

DISCUSSION

In this work, we demonstrate the specificity of physical interactions between *E. coli* GrxD, NfuA, and an FeS cluster client protein, the sulfur-donating radical AdoMet enzyme MiaB. Moreover, we report that NfuA is capable of intact FeS cluster transfer to apo-MiaB, whereas GrxD is not, and implicate both of these factors as working synergistically to maintain MiaB activity in the cell. Recent work based on *in vitro* FeS cluster transfer experiments has suggested that monothiol glutaredoxins may act as FeS cluster shuttles (13), perhaps acting to transfer clusters to (or between) A-type carrier proteins. This work does not address the potential for GrxD to act in cluster transfer between A-type carrier proteins, but demonstrates for the first time a role for GrxD in the *in vivo* activity of an FeS client protein. Moreover, we also report the first quantitative interaction data for the final step in FeS protein maturation, the association of an FeS carrier protein and an apo-FeS client protein. The quantitative binding data for the MiaB/NfuA interaction (Fig. 3*B*) are in good agreement with the data of the AcnB/NfuA interaction, from which aconitase B had previously been established as an NfuA client protein (8).

The members of the radical AdoMet superfamily are FeS cluster-dependent enzymes that use *S*-adenosylmethionine to perform a wide diversity of reactions, including the functionalization of inert C–H bonds (30). A small subset of these enzymes is able to catalyze the formation of C–S bonds. *E. coli* encodes four such enzymes: the biotin synthase, BioB (31), the lipoic acid synthase, LipA (32), the ribosomal protein-modifying enzyme, RimO (33), and the tRNA-modifying enzyme, MiaB (18). Radical AdoMet enzymes such as MiaB require the sacrifice of an auxiliary FeS cluster as a source of sulfur to perform their catalytic cycles (22). In the case of MiaB, studies hypothesized that an iron sulfur cluster located in the N-terminal part of the enzyme (a UPF0004 domain) would be a sacrificial sulfur donor to perform the sulfur insertion reaction followed by a methylation reaction (21). Even in the presence of cysteine and cysteine desulfurase, no more than one turnover had been obtained for MiaB *in vitro*, suggesting that an as yet uncharacterized repair mechanism is required (25).

We found that GrxD and NfuA can interact with MiaB using multiple methods such as affinity co-purification, SPR, and gel filtration. Affinity co-purification and SPR indicated that MiaB interacts specifically with GrxD and NfuA as all the other A-type carriers from *E. coli* such as SufA, IscA, and ErpA did not interact with MiaB (Fig. 2). Affinity co-purification experiments were enriched with quantitative data obtained by SPR. To our knowledge, the only studies with quantitative data characterizing the interactions involving FeS cluster biosynthesis factors were between SufS/SufE and SufE/SufBCD (34) and between IscS/IscU (35). Both of these studies indicated an interaction in the low micromolar range (2 μM for IscS/IscU, 0.36 μM for SufS/SufE, and 2.78 μM for SufE/SufBCD). It should be noted that these associations represent what are believed to be highly specific interactions within and between cysteine desulfurase subunits and their cognate primary scaffold proteins. No quantitative data are available characterizing downstream interactions between scaffold proteins and A-type carrier proteins or between carrier proteins and (apo)-FeS client proteins.

Our SPR results indicated that MiaB interacts with GrxD with a K_D of 12.0 ± 2.6 μM (Fig. 3*A*) and with NfuA with a K_D of 44.0 ± 5.2 μM (Fig. 3*B*). We believe these affinities are compatible with an *in vivo* function when one considers the increased putative substrate range of carrier proteins where a handful of factors may be responsible for maturation of at least 110 FeS proteins (1). We should note that as these measures were made using proteins in their apo form, it is possible that these affinities could be modulated by the presence of an FeS cluster. Indeed, recent work studying the interaction between NfuA and AcnB showed that NfuA was preferentially interacting with an apo form of AcnB, although no quantitative data were reported (8). As a *bona fide* client substrate of NfuA, we established the K_D for the AcnB/NfuA interaction to be 54.6 ± 8.3 μM (Fig. 3*C*). These data are in close agreement with the data obtained for MiaB and reinforce the physiological relevance of such interactions. Small amounts of MiaB were previously observed to co-purify with BolA via affinity purification (10, 14). In light of the data presented here, we now believe that the presence of MiaB in these pulldown experiments was due to its association with GrxD, perhaps as a component of a GrxD-BolA heterodimer (10). The weak signal suggesting a BolA/

MiaB interaction from affinity co-purification (Fig. 2) was not reproduced using SPR (data not shown). The interaction observed during the co-purification experiment is therefore likely an artifact of a nonspecific interaction and reinforces the necessity to use multiple methods to measure interactions.

A commonly used approach when characterizing FeS cluster scaffold and carrier proteins is to assess their capacity to transfer FeS clusters, intact, to partner carriers or model FeS client apoproteins (8, 16, 17). Indeed, the *in vitro* transfer of an FeS cluster from *A. vinelandii* IscU scaffold protein to the monothiol glutaredoxin *A. vinelandii* Grx5 and the transfer of an FeS cluster from *A. vinelandii* Grx-nif (among others) to the *A. vinelandii* ^{Nif}IscA carrier protein have recently been reported (13, 36). Likewise, Py *et al.* (8) reported the *in vitro* transfer of FeS clusters from SufA and IscA to NfuA. These transfer reactions were monitored spectroscopically, and no physical interaction data, qualitative or quantitative, were reported for the donor and recipient proteins. Indeed, remarkable plasticity was observed and rapid cluster transfer was noted from *Arabidopsis thaliana* GrxS14 and *Saccharomyces cerevisiae* Grx3 to *A. vinelandii* ^{Nif}IscA. This plasticity may suggest that *in vitro* FeS cluster transfer reactions are driven largely by thermodynamics and, in the absence of additional physical and functional interaction data, cannot alone document physiologically relevant associations. With this caveat in mind, our observation of a physical interaction and quasi-stable complex formation (Fig. 6*A*) between MiaB and NfuA indicates that *in vitro* FeS transfer from NfuA to MiaB is likely to be physiologically relevant (Fig. 6, *B–D*). Moreover, even in the absence of observed cluster transfer from holo-GrxD to apo-MiaB, which is perhaps not surprising given the capacity of GrxD to bind a 2Fe2S cluster and the presence of only 4Fe4S clusters in holo-MiaB, the specific and quantitative physical interaction of GrxD (apo and holo) with MiaB supports a functional interaction between these proteins (Figs. 3 and 5).

To reconcile *in vitro* interaction and transfer data with function, we assayed the *in vivo* activity of MiaB in various mutant backgrounds by monitoring levels of tRNA modification, namely the ratios of i^6A to ms^2i^6A (Fig. 7*A*). Quantification of i^6A and ms^2i^6A indicated that *grxD* and *nfuA* single mutants do not display major defects in ms^2i^6A production, perhaps due to partial functional redundancy and additional compensating factors within the cell. However, in stark contrast, an *nfuA/grxD* double mutant displayed a major decrease in ms^2i^6A when compared with i^6A. This indicates that both GrxD and NfuA are important in maintaining the *in vivo* activity of MiaB.

As severe lack of tRNA modification is seen only in the double mutant, a simple hypothesis could be that NfuA and GrxD are functionally redundant. We do not believe this functional redundancy is at the molecular level, however, as *in vitro* biochemical data indicate different properties for intact cluster transfer from these factors to MiaB. Our current favored hypothesis is that GrxD and NfuA are functionally redundant at the level of "maintaining MiaB activity" and fulfill different functions with MiaB, such as *de novo* FeS cluster insertion and FeS cluster repair or regeneration. We have illustrated a putative model for the interactions and functions of GrxD and NfuA with MiaB (Fig. 8).

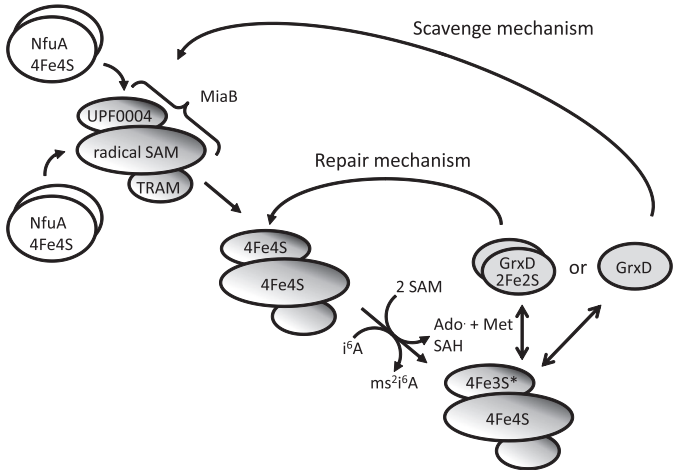

FIGURE 8. **Proposed model for the interaction of MiaB with GrxD and NfuA.** MiaB is composed of three main domains, a TRAM domain that binds a substrate tRNA molecule, a radical SAM domain that binds an AdoMet molecule as well as a 4Fe4S cluster, and a UPF0004 domain containing the sacrificial substrate 4Fe4S cluster. NfuA can interact with and transfer 4Fe4S clusters to both radical SAM and UPF0004 domains in apo-MiaB. Once MiaB is loaded with two FeS clusters, the enzyme is able to methylthiolate its tRNA targets (*i6A*) using two molecules of AdoMet (producing a 5′-deoxyadenosyl radical, *Ado.*, methionine, *Met*, and *S*-adenosyl-*L*-homocysteine, *SAH*) and a sulfur atom, most likely sourced from the UPF0004 domain 4Fe4S cluster and resulting in the presence of a modified tRNA (*ms2i6A*) and a partially degraded cluster (shown as *4Fe3S*). To perform another turnover, this substrate cluster requires regeneration either via direct repair or via "scavenge and replace" mechanism. In the case of a direct repair mechanism, a GrxD homodimer could sacrifice its 2Fe2S cluster to replace the missing sulfur atom in MiaB. If a scavenge and replace mechanism occurs, GrxD could accept the used substrate cluster from MiaB, regenerating an empty UPF0004 domain, a target for *de novo* cluster insertion by NfuA.

Based on data reported here, NfuA is a strong candidate to be the major physiological provider of both 4Fe4S clusters present in radical SAM and UPF0004 domains of apo-MiaB *in vivo*. The role of GrxD is more speculative, but may be centered around the repair or regeneration of the UPF0004 domain substrate FeS cluster during MiaB turnover. This substrate FeS cluster present after turnover is annotated as a 4Fe3S cluster in the model, but has never been observed and remains to be characterized. As presented in the model, we believe that holo-GrxD could bind and repair the used substrate FeS cluster in the UPF0004 domain, recreating the active form of MiaB. Alternatively, apo-GrxD could scavenge the remaining used substrate FeS cluster, generating holo-GrxD and an empty UPF0004 domain ready for a fresh round of *de novo* cluster insertion by NfuA. Either function of repair or scavenging by GrxD would likely make regeneration of the catalytically competent form of MiaB more efficient. From a cellular perspective, the absence of GrxD may therefore slow down MiaB turnover, but could potentially be compensated for by increased levels of MiaB in the cell (or increased levels of MiaB synthesis and degradation). This could explain the observed lack of an effect on MiaB activity in a *grxD* null mutant. Likewise, lack of NfuA in the cell does give rise to a small MiaB activity defect, but is likely compensated for by increased regeneration of MiaB enzyme, by GrxD, and by *de novo* cluster insertion into apo-MiaB directly by scaffold proteins (IscU, SufBCD) or other as yet unidentified factors. Only in the *nfuA*/*grxD* double mutant where both a major *de novo* biosynthesis factor and a major regeneration factor are

absent is a large defect in MiaB activity observed. The observation of some MiaB activity in an *nfuA/grxD* double mutant supports a potential minor role for other unidentified factors in MiaB maturation.

We believe that the observed synergistic effect of GrxD and NfuA is larger in scope than MiaB alone, and evidence to support this is provided by growth studies (Fig. 7*B*). The growth curves reported show that an *miaB* null mutant grows significantly faster than an *nfuA*/*grxD* null mutant, indicating that in addition to being involved in MiaB activity, GrxD and NfuA affect the function of other cellular processes. The observation of an aggravating genetic interaction between *grxD* and *nfuA* mutations is congruous with the hypothesis that these factors may fulfill primarily different roles with client proteins. Future work will explore the interactions of GrxD and NfuA with MiaB and their impact on other cellular processes.

Acknowledgments—We thank Nancy Liu, Jennifer He, and Marjon Khairy for the construction of E. coli mutants. We thank M. Dong (Lawrence Berkeley National Laboratory, Berkeley, CA) and P. Hwang (University of California, San Francisco, CA) for critical reading of the manuscript. We also thank A. W. Hill (GE Healthcare) and R. Latvala (GE Healthcare) for technical assistance and helpful discussions with SPR experiments.

REFERENCES

1. Fontecave, M. (2006) Iron-sulfur clusters: ever-expanding roles. *Nat. Chem. Biol.* **2,** 171–174
2. Py, B., and Barras, F. (2010) Building Fe-S proteins: bacterial strategies. *Nat. Rev. Microbiol.* **8,** 436–446
3. Rouault, T. A. (2012) Biogenesis of iron-sulfur clusters in mammalian cells: new insights and relevance to human disease. *Dis. Model Mech.* **5,** 155–164
4. Lill, R. (2009) Function and biogenesis of iron-sulphur proteins. *Nature* **460,** 831–838
5. Shepard, E. M., Boyd, E. S., Broderick, J. B., and Peters, J. W. (2011) Biosynthesis of complex iron-sulfur enzymes. *Curr. Opin. Chem. Biol.* **15,** 319–327
6. Pinske, C., and Sawers, R. G. (2012) A-type carrier protein ErpA is essential for formation of an active formate-nitrate respiratory pathway in *Escherichia coli* K-12. *J. Bacteriol.* **194,** 346–353
7. Pinske, C., and Sawers, R. G. (2012) Delivery of iron-sulfur clusters to the hydrogen-oxidizing [NiFe]-hydrogenases in *Escherichia coli* requires the A-type carrier proteins ErpA and IscA. *PLoS One* **7,** e31755
8. Py, B., Gerez, C., Angelini, S., Planel, R., Vinella, D., Loiseau, L., Talla, E., Brochier-Armanet, C., Garcia Serres, R., Latour, J. M., Ollagnier-de Choudens, S., Fontecave, M., and Barras, F. (2012) Molecular organization, biochemical function, cellular role and evolution of NfuA, an atypical Fe-S carrier. *Mol. Microbiol.* **86,** 155–171
9. Butland, G., Babu, M., Díaz-Mejía, J. J., Bohdana, F., Phanse, S., Gold, B., Yang, W., Li, J., Gagarinova, A. G., Pogoutse, O., Mori, H., Wanner, B. L., Lo, H., Wasniewski, J., Christopolous, C., Ali, M., Venn, P., Safavi-Naini, A., Sourour, N., Caron, S., Choi, J. Y., Laigle, L., Nazarians-Armavil, A., Deshpande, A., Joe, S., Datsenko, K. A., Yamamoto, N., Andrews, B. J., Boone, C., Ding, H., Sheikh, B., Moreno-Hagelseib, G., Greenblatt, J. F., and Emili, A. (2008) eSGA: *E. coli* synthetic genetic array analysis. *Nat. Methods* **5,** 789–795
10. Yeung, N., Gold, B., Liu, N. L., Prathapam, R., Sterling, H. J., Willams, E. R., and Butland, G. (2011) The *E. coli* monothiol glutaredoxin GrxD forms homodimeric and heterodimeric FeS cluster containing complexes. *Biochemistry* **50,** 8957–8969
11. Li, H., Mapolelo, D. T., Randeniya, S., Johnson, M. K., and Outten, C. E. (2012) Human glutaredoxin 3 forms [2Fe-2S]-bridged complexes with human BolA2. *Biochemistry* **51,** 1687–1696
12. Santos, J. M., Lobo, M., Matos, A. P., De Pedro, M. A., and Arraiano, C. M. (2002) The gene *bolA* regulates dacA (PBP5), dacC (PBP6), and ampC (AmpC), promoting normal morphology in *Escherichia coli*. *Mol. Microbiol.* **45,** 1729–1740
13. Mapolelo, D. T., Zhang, B., Randeniya, S., Albetel, A. N., Li, H., Couturier, J., Outten, C. E., Rouhier, N., and Johnson, M. K. (2013) Monothiol glutaredoxins and A-type proteins: partners in Fe-S cluster trafficking. *Dalton Trans.* **42,** 3107–3115
14. Butland, G., Peregrín-Alvarez, J. M., Li, J., Yang, W., Yang, X., Canadien, V., Starostine, A., Richards, D., Beattie, B., Krogan, N., Davey, M., Parkinson, J., Greenblatt, J., and Emili, A. (2005) Interaction network containing conserved and essential protein complexes in *Escherichia coli*. *Nature* **433,** 531–537
15. Pierrel, F., Björk, G. R., Fontecave, M., and Atta, M. (2002) Enzymatic modification of tRNAs: MiaB is an iron-sulfur protein. *J. Biol. Chem.* **277,** 13367–13370
16. Angelini, S., Gerez, C., Ollagnier-de Choudens, S., Sanakis, Y., Fontecave, M., Barras, F., and Py, B. (2008) NfuA, a new factor required for maturing Fe/S proteins in *Escherichia coli* under oxidative stress and iron starvation conditions. *J. Biol. Chem.* **283,** 14084–14091
17. Bandyopadhyay, S., Naik, S. G., O'Carroll, I. P., Huynh, B. H., Dean, D. R., Johnson, M. K., and Dos Santos, P. C. (2008) A proposed role for the *Azotobacter vinelandii* NfuA protein as an intermediate iron-sulfur cluster carrier. *J. Biol. Chem.* **283,** 14092–14099
18. Esberg, B., Leung, H. C., Tsui, H. C., Björk, G. R., and Winkler, M. E. (1999) Identification of the *miaB* gene, involved in methylthiolation of isopentenylated A37 derivatives in the tRNA of *Salmonella typhimurium* and *Escherichia coli*. *J. Bacteriol.* **181,** 7256–7265
19. Pierrel, F., Douki, T., Fontecave, M., and Atta, M. (2004) MiaB protein is a bifunctional radical-*S*-adenosylmethionine enzyme involved in thiolation and methylation of tRNA. *J. Biol. Chem.* **279,** 47555–47563
20. Pierrel, F. (2003) MiaB protein from *Thermotoga maritima*: Characterization of an extremely thermophilic tRNA-methylthiotransferase. *J. Biol. Chem.* **278,** 29515–29524
21. Atta, M., Arragain, S., Fontecave, M., Mulliez, E., Hunt, J. F., Luff, J. D., and Forouhar, F. (2012) The methylthiolation reaction mediated by the radical-SAM enzymes. *Biochim. Biophys. Acta* **1824,** 1223–1230
22. Lanz, N. D., and Booker, S. J. (2012) Identification and function of auxiliary iron-sulfur clusters in radical SAM enzymes. *Biochim. Biophys. Acta* **1824,** 1196–1212
23. Baba, T., Ara, T., Hasegawa, M., Takai, Y., Okumura, Y., Baba, M., Datsenko, K. A., Tomita, M., Wanner, B. L., and Mori, H. (2006) Construction of *Escherichia coli* K-12 in-frame, single-gene knockout mutants: the Keio collection. *Mol. Syst. Biol.* **2,** 2006.0008
24. Datsenko, K. A., and Wanner, B. L. (2000) One-step inactivation of chromosomal genes in *Escherichia coli* K-12 using PCR products. *Proc. Natl. Acad. Sci. U.S.A.* **97,** 6640–6645
25. Hernández, H. L., Pierrel, F., Elleingand, E., García-Serres, R., Huynh, B. H., Johnson, M. K., Fontecave, M., and Atta, M. (2007) MiaB, a bifunctional radical-*S*-adenosylmethionine enzyme involved in the thiolation and methylation of tRNA, contains two essential [4Fe-4S] clusters. *Biochemistry* **46,** 5140–5147
26. Gao-Sheridan, H. S., Pershad, H. R., Armstrong, F. A., and Burgess, B. K. (1998) Discovery of a novel ferredoxin from *Azotobacter vinelandii* containing two [4Fe-4S] clusters with widely differing and very negative reduction potentials. *J. Biol. Chem.* **273,** 5514–5519
27. Ranquet, C., Ollagnier-de-Choudens, S., Loiseau, L., Barras, F., and Fontecave, M. (2007) Cobalt stress in *Escherichia coli*: the effect on the iron-sulfur proteins. *J. Biol. Chem.* **282,** 30442–30451
28. Waller, J. C., Ellens, K. W., Hasnain, G., Alvarez, S., Rocca, J. R., and Hanson, A. D. (2012) Evidence that the folate-dependent proteins YgfZ and MnmEG have opposing effects on growth and on activity of the iron-sulfur enzyme MiaB. *J. Bacteriol.* **194,** 362–367
29. Waller, J. C., Alvarez, S., Naponelli, V., Lara-Nuñez, A., Blaby, I. K., Da Silva, V., Ziemak, M. J., Vickers, T. J., Beverley, S. M., Edison, A. S., Rocca, J. R., Gregory, J. F., 3rd, de Crécy-Lagard, V., and Hanson, A. D. (2010) A role for tetrahydrofolates in the metabolism of iron-sulfur

clusters in all domains of life. *Proc. Natl. Acad. Sci. U.S.A.* **107,** 10412–10417
30. Booker, S. J. (2009) Anaerobic functionalization of unactivated C–H bonds. *Curr. Opin. Chem. Biol.* **13,** 58–73
31. Ugulava, N. B., Frederick, K. K., and Jarrett, J. T. (2003) Control of adenosylmethionine-dependent radical generation in biotin synthase: a kinetic and thermodynamic analysis of substrate binding to active and inactive forms of BioB. *Biochemistry* **42,** 2708–2719
32. Cicchillo, R. M., Iwig, D. F., Jones, A. D., Nesbitt, N. M., Baleanu-Gogonea, C., Souder, M. G., Tu, L., and Booker, S. J. (2004) Lipoyl synthase requires two equivalents of *S*-adenosyl-L-methionine to synthesize one equivalent of lipoic acid. *Biochemistry* **43,** 6378–6386
33. Lee, K. H., Saleh, L., Anton, B. P., Madinger, C. L., Benner, J. S., Iwig, D. F., Roberts, R. J., Krebs, C., and Booker, S. J. (2009) Characterization of RimO, a new member of the methylthiotransferase subclass of the radical SAM superfamily. *Biochemistry* **48,** 10162–10174
34. Layer, G., Gaddam, S. A., Ayala-Castro, C. N., Ollagnier-de Choudens, S., Lascoux, D., Fontecave, M., and Outten, F. W. (2007) SufE transfers sulfur from SufS to SufB for iron-sulfur cluster assembly. *J. Biol. Chem.* **282,** 13342–13350
35. Urbina, H. D., Silberg, J. J., Hoff, K. G., and Vickery, L. E. (2001) Transfer of sulfur from IscS to IscU during Fe/S cluster assembly. *J. Biol. Chem.* **276,** 44521–44526
36. Shakamuri, P., Zhang, B., and Johnson, M. K. (2012) Monothiol glutaredoxins function in storing and transporting [Fe2S2] clusters assembled on IscU scaffold proteins. *J. Am. Chem. Soc.* **134,** 15213–15216